Published in final edited form as:

Biochim Biophys Acta. 2016 January ; 1863(1): 115–127. doi:10.1016/j.bbamcr.2015.10.016.

WHIRLIN INCREASES TRPV1 CHANNEL EXPRESSION AND CELLULAR STABILITY

Maria Grazia Ciardo[1,2], **Amparo Andrés-Bordería**[2], **Natalia Cuesta**[1], **Pierluigi Valente**[1], **María Camprubí-Robles**[1], **Jun Yang**[3], **Rosa Planells-Cases**[2,*], and **Antonio Ferrer-Montiel**[1,*]

[1]Instituto de Biología Molecular y Celular. Universitas Miguel Hernández, Alicante, Spain

[2]Centro de Investigaciones Príncipe Felipe. Valencia. Spain

[3]John A Moran Eye Center. The University of Utah. Salt Lake City, Utah 84132. USA

Abstract

The expression and function of TRPV1 is influenced by its interaction with cellular proteins. Here, we identify whirlin, a cytoskeletal PDZ-scaffold protein implicated in hearing, vision and mechanosensory transduction, as an interacting partner of TRPV1. Whirlin associates with TRPV1 in cell lines and in primary cultures of rat nociceptors. Whirlin is expressed in 55% of mouse sensory C-fibers, including peptidergic and non-peptidergic nociceptors, and co-localizes with TRPV1 in 70% of them. Heterologous expression of Whirlin increased TRPV1 protein expression and trafficking to the plasma membrane, and promoted receptor clustering. Silencing Whirlin expression with siRNA or blocking protein translation resulted in a concomitant degradation of TRPV1 that could be prevented by inhibiting the proteasome. The degradation kinetics of TRPV1 upon arresting protein translation mirrored that of Whirlin in cells co-expressing both proteins, suggesting a parallel degradation mechanism. Noteworthy, Whirlin expression significantly reduced TRPV1 degradation induced by prolonged exposure to capsaicin. Thus, our findings indicate that Whirlin and TRPV1 are associated in a subset of nociceptors and that TRPV1 protein stability is increased through the interaction with the cytoskeletal scaffold protein. Our results suggest that the Whirlin-TRPV1 complex may represent a novel molecular target and its pharmacological disruption might be a therapeutic strategy for the treatment of peripheral TRPV1-mediated disorders.

Keywords

nociception; thermosensory; PDZ; synapsis; cytoskeleton; pain

[*]To whom correspondence should be addressed: Antonio Ferrer-Montiel, aferrer@umh.es or Rosa Planells-Cases, Rosa.Planells-Cases@mdc-berlin.de.

Conflict of interest. The authors declare no conflict of interest.

1. Introduction

Transient receptor potential vanilloid 1 (TRPV1) is a thermosensory channel activated by physical and chemical stimuli (1). This ion channel was initially described as the sensor for noxious temperatures (>42°C) and vanilloid molecules such as capsaicin (2). TRPV1 is also gated by very strong membrane depolarization, and its gating mechanism can be potentiated by mild extracellular acidification (3,4). A hallmark of TRPV1 activity is its significant potentiation by pro-algesic agents released upon tissue injury or inflammation (5). This potentiation is produced by alteration of the channel gating mechanism by chemical modification of the protein (6), and/or by enhancing the recruitment of new channels to the plasma membrane through regulated exocytosis of receptors stored in large-dense core vesicles (7). The pivotal role in the onset, setting and maintenance of nociceptor inflammatory sensitization has signaled TRPV1 as a valuable therapeutic target for pain intervention (8), leading to the implementation of a plethora of drug discovery programs that have provided a myriad of channel antagonists (9). However, none of these molecules has been developed clinically yet because of unwanted side effects arising from extensive blockade of the receptor (10).

Structurally, TRPV1 is a homomeric integral membrane protein displaying the assembly of four identical subunits around a central axis of symmetry centered in the channel pore (11). Each subunit contains 6-transmembrane segments, of which S5 and S6 structure the walls of the permeation pathway, while the other segments contribute to design part of the gating sensors (12). In addition, each subunit contains a cytosolic C-terminal domain that has been involved in regulating the association of subunits and channel gating (13,14). Furthermore, the N-terminus is also a cytosolic domain that displays the presence of several ankyrin domains, which mediate the interaction with cellular proteins thus contributing to define the activity of the thermosensory channel, either by modulating its gating properties (15), or its trafficking, insertion and clustering into the plasma membrane (16).

Noteworthy, it is becoming clear that ion channels are not isolated molecular devices but rather components of protein complexes, that through orchestrated interactions contribute to define their signaling in a time- and context-dependent manner (17). Thus, elucidating the molecular components of the TRPV1 “signalplex” is becoming central to understand the contribution of this thermoTRP to thermal sensation as well as to nociceptor sensitization under pathological conditions. To identify interacting TRPV1 proteins, we used the yeast two-hybrid approach to screen a cDNA neuronal library using the N-terminus domain of TRPV1 (NtTRPV1) as bait. Our screening identified the cytoskeletal PDZ-scaffold protein Whirlin, also known as Calmodulin-dependent Serine Kinase (CASK)-interacting protein of 98 kDa (CIP98) (18), as a putative TRPV1 interacting partner. Whirlin has three Class I PDZ domains (19), two located in the N-terminus and a Proline-rich region at the C-terminus, between the second and third PDZ domains (20). Whirlin was initially identified as a protein that interacts with CASK, a member of the Membrane-Associated Guanylate Kinase (MAGUK) that plays an important role in synaptic development and plasticity (21). Notably, in humans Whirlin is encoded by the Deafness Autosomal Recessive 31 (DFNB31) locus. Genetic defects in the Whirlin gene cause non-syndromic deafness and the Usher2 syndrome (22,23). Recently, a role in mechanosensory signaling has also been uncovered for

Whirlin consistent with its expression in mammalian proprioceptors (24). Collectively, all these data imply a central role of Whirlin in hearing, vision and in sensory transduction.

Here, we show that Whirlin interacts with TRPV1 in transfected cell lines and in DRG neurons. Noteworthy, TRPV1 associates with long and short isoforms of Whirlin. Heterologous co-expression of Whirlin with TRPV1 increases the total and membrane expression of the vanilloid receptor. This enhanced channel expression is not translated into higher channel function because of receptor clustering in the cell membrane. Conversely, silencing of Whirlin expression using specific siRNA decreased the level of TRPV1 cellular expression and reduced channel activity. This effect was prevented by inhibition of the proteasome that inhibits Whirlin and TRPV1 degradation. Noteworthy, in cells co-expressing TRPV1 and Whirlin the kinetics of TRPV1 proteasomal degradation paralleled that of Whirlin, and the PDZ-scaffold protein reduced TRPV1 internalization and degradation due to prolonged exposure to capsaicin. Taken together, our findings indicate that Whirlin complexes with TRPV1 and stabilizes its cellular and membrane expression.

2. Materials and methods

2.1 Chemicals and Antibodies

All drugs were from Sigma (St. Louis, MO, USA) unless otherwise stated. Anti-Whirlin serum (Genscript Corporation), polyclonal anti-Whirlin (Abcam), anti-TRPV1 serum (16), polyclonal anti-TRPV1 (Alomone Labs Ltd, Chemicon), anti-TRPV1 extracellular (α-TRPV1e) (7), rabbit anti-Neurofilament 200, Isolectin B4-Alexa 568 (Molecular Probes) and goat anti-CGRP (Abcam) were used. Secondary antibodies were from Jackson ImmunoResearch Laboratories.

2.2 Yeast two-hybrid screen

The yeast 2-hybrid screen was performed with the cytosolic N-terminal domain of TRPV1 (NtTRPV1), as previously described (16).

2.3 Plasmids and deletions

Human Whirlin cDNA (Open Biosystems) was subcloned in pcDNA3.1-Myc-His plasmid (Invitrogen) for eukaryotic expression. The cytosolic NtTRPV1 domain was cloned in pGEX-4T-1 vector (GE Healthcare) to be expressed as a GST-fusion protein. The truncated form TRPV1-VStop was obtained by introducing a stop codon at position Val-828. The HA-TRPV1 and YFP-TRPV1 used were described previously (13,25).

2.4 Animal models

All experimental procedures were approved by the Institutional Animal and Ethical Committee of the University Miguel Hernandez de Elche and in accordance with the guidelines of the Economic European Community. Neonatal Wistar rats and wild-type C57BL/6J mice (in house-bred stock originally from Harlan Laboratories). Whirler mice were kindly provided by Dr. P. Mburu (20). Genetically, the mutation in the Whirler mice consists of a 592 bp deletion that leads to a truncation of the long isoform before the third PDZ and encompasses the first methionine of the short isoform. Whirlin$^{neo/neo}$ mice are

transgenic mice that do not express the long isoform of the PDZ protein, and were obtained as described (26).

2.5 Genotyping

Genomic DNA was extracted from mice tails. For whirler mice, primer sequences and cycling conditions for PCR were obtained from Dr. Mburu's lab as follows: TGGCCAACCTCTGTGCTTCC (D4Mit17) and ACAGTTGTCCTCTGACATCC (D4Mit17 rev), resulting in 144 bp band for wild type; CAAAATATCTGACAAAAACAAGTGTG (D4Mit244) and GGTGTCATCACCATGATGGA (D4Mit244 rev), resulting in 144 bp band for wild type and two 130/110 bands for Whirler. Cycling conditions used were: 95°C for 5 min and 35 cycles of (95°C for 30 sec, 68°C for 1.5 min), and 68°C for 3 min. 94°C for 3′, 35 cycles of (94°C for 2′, 58°C for 1′, 68°C for 2′). For Whirlin$^{neo/neo}$ mice, primer sequences and cycling conditions were as described (27).

2.6 Cell Culture

Primary cultures of neonatal rat or adult mice DRG neurons were prepared as in (7,28) respectively. Human embryonic kidney cells (HEK293) and a hybridoma of the mouse neuroblastoma cell line N18TG-2 and embryonic rat DRGs (F11 cells), were cultured as previously described (29,30) and used 48 h after transfection with JetPeI™ (Polysciences) or Lipofectamine™ (Invitrogen) following the manufacturer's instructions.

For DRGs electroporation, the Neon transfection system (Invitrogen) was used following manufacturer's instructions. Neurons were extracted from neonatal rats and after digestion with collagenase, they were resuspended in 10 μl of resuspension buffer plus 1 μg cDNA per reaction (Whirlin or YFP as control). Two pulses of 20 ms at 1,200V were applied and cells then resuspended and seeded in complete medium without antibiotics for 3–4 hours before changing to complete medium.

2.7 Short interfering RNA

Three different siRNAs (Ambion) were used to suppress Whirlin expression in F11 and DRGs cultures: C1 (CGAUAAAUCUCUAGCCCGG, chromosome 5-587 in exon 1), C2 (GGAUUUACAAGGGCCCAG, chromosome 5-1212 in exon 6), C3 (CCAUGAUGUACUACCUAGA, chromosome 5-1327 in exon 6). A scrambled siRNA (a siRNA with a random sequence) was also used as negative control.

As the three siRNAs recognized species-specific sequences from the Rattus Norvegicus ortholog of Whirlin (NCBI Reference Sequence: NM_181088), this was isolated by PCR from a rat brain cDNA library (16), and subsequently subcloned in the pcDNA 3.1-Myc-His plasmid. The resulting plasmid was cotransfected with TRPV1 in F11 cells in presence of either of the siRNAs described above.

2.8 Quantitative real time PCR

Total RNA was isolated from rat DRGs using E.Z.N.A.™ HP Total RNA Kit (Omega). RNA concentration was estimated and 1 μg RNA was used for reverse transcription with Gene

Amp® RNA PCR (Applied Byosistems), according to the manufacturer conditions. Quantitative real time PCR (qPCR) was performed with 20 ng cDNA using appropriate Taqman® for rat Whirlin (Reference number 00710383_m1, Applied Biosystems) and Taqman PCR Mastermix (Applied Biosystems). Three replicate for each sample were tested. Singleplex reactions were runned with an ABI PRISM 7700 thermocycler (Applied Byosystems) using the following cycling conditions: 50°C for 2 minutes; 95°C for 10 minutes; 40 cycles of (95°C for 15 seconds; 60°C for 1 minute). A non-template sample was used as a control.

2.9 *In vitro* Pull-down assay

GST fusion proteins were in-batch affinity purified on glutathione-Sepharose 4B (GE Healthcare). HEK293 cells were transfected with myc-tagged Whirlin (Whirlin-myc) cDNA and cultured for 48 h. Immobilized GST-NtTRPV1 domain or GST as control were incubated overnight at 4°C with HEK293 myc-tagged Whirlin extracts in buffer (containing in mM: 100 NaCl; 10 $MgCl_2$; 10 Tris; 5 EDTA, pH 7.5; 1% Triton X-100 and 0.5% NP-40). After several washes with same buffer, protein complexes were eluted, denatured, and resolved by SDS/PAGE.

2.10 Co-immunoprecipitation

HEK293 cells co transfected with the TRPV1 wild type or VStop and Whirlin-myc or PSD95-myc were solubilized in RIPA buffer (50 mM Tris-Cl pH 7.4, 150 mM NaCl, 1% NP-40, 0.5% sodium deoxycholate, 0.1% SDS) containing proteases inhibitors. The solubilized supernatants (~900 μg of protein) were incubated overnight at 4°C with 10 μl of anti-c-Myc agarose (Pierce). Immunocomplexes were washed three times with a solution of TBS plus 0.05% Tween-20, eluted with SDS sample buffer and analyzed by immunoblotting.

2.11 Biotin labelling of surface proteins

HEK293 cells transiently coexpressing TRPV1 plus Whirlin-myc (or plus YFP in control) were incubated with 0.5 mg/ml sulfo-NHS-SS-Biotin (Pierce) for 30 min at 4°C. Plates were rinsed with Tris 10 mM pH 7.4, 150 mM NaCl and incubated in the same buffer for 30 min at 4°C to quench unreacted biotin. Cells were lysed for 1 h at 4°C with lysis buffer (50 mM Hepes pH 7.4; 140 mM NaCl; 10% Glycerol; 1% Triton X-100; 1 mM EDTA; 2 mM EGTA; 0.5% Deoxycholate) containing proteases inhibitors. Biotin-labeled proteins were isolated incubating cell lysates with streptavidin agarose overnight at 4°C. Isolated fractions were resolved by SDS-PAGE.

2.12 Immunocytochemistry

Primary DRGs cultures were fixed, blocked, permeabilized and subsequently incubated with both guinea pig anti-capsaicin receptor antibody (Chemicon) and anti-Whirlin serum (Genscript) or polyclonal antibody (Abcam). HEK293 cells were co-transfected with TRPV1 plus Whirlin-myc (or plus DsRed in control) and cultured 48 h before incubation 1 h at 4°C with rabbit anti-rat TRPV1 extracellular (Alomone Labs Ltd), a TRPV1 antibody that specifically recognizes an extracellular epitope (7). After several washes, cells were fixed,

permeabilized and thereafter incubated overnight at 4°C with mouse anti-c-myc. After extensive washing cells were incubated with the secondary antibodies, mounted and analyzed by confocal microscopy (Leica TCS).

2.13 Immnohistochemistry

Mice were over-anesthetized with pentobarbital (50 mg/kg, i.p. in saline) and then transcardially perfused through the left ventricle with cold saline followed by 4% PFA in PBS (pH 7.4). Isolated DRGs were post-fixed for 4 h in the same fixative solution at 4°C, immersed in sucrose gradient solutions (10, 20, and 30%) in PBS for cryoprotection until the tissues sunk and then frozen with dryice in mounting medium (OCT.™, Tissue-Tek). DRGs were serially cut at 14 μm thickness on a cryostat, mounted onto polylysine-coated Menzel-Gläser Superfrost UltraPlus® slides (Thermos Scientific), and kept at −20°C until use. Slides were then defrosted, washed, blocked/permeabilized with 10% normal goat or donkey serum, 3% BSA and 0.3% Triton X-100 in PBS and incubated o/n at 4°C with the primary antibodies diluted in the blocking solution. After washing with PBS-Tween 0.05%, sections were incubated with the appropriate secondary antibodies (1 h at RT) and mounted with Mowiol® (Calbiochem). Cell nuclei stained with DAPI (300 nM in PBS, 5 min, RT) (Molecular Probes, Invitrogen). Sample images were captured with an inverted confocal microscope (Zeiss LSM 5 Pascal, Carl Zeiss, 40× objective) and then analyzed with Zen Lite 2012 software (Zeiss) under blinded conditions to determine the percentage of TRPV1 or Whirlin positive neurons that were also positive for CGRP, IB4 or NF200 markers (referred to as $TRPV1^+ \times marker^+$ or $Whirlin^+ \times marker^+$). More than five sections per animal, three mice, and >1000 total neurons per group were analyzed. Data expressed as means±SEM. and statistical analysis performed by two-way ANOVA, followed by Bonferroni post-test. Significance level was preset to $p<0.05$.

2.14 Ca^{2+} imaging

HEK293 cells cotransfected with TRPV1 and Whirlin-myc, or pcDNA in control, were loaded with 5 μM fluo-4-acetoxymethyl ester (Fluo-4-AM, Molecular Probes) in the presence of 0.02% pluronic F-127 acid (Invitrogen) in Hank's balanced salt solution (HBSS) (140 mM NaCl, 4 mM KCl, 1 mM $MgCl_2$, 1.8 mM $CaCl_2$, 5 mM D-glucose, 10 mM HEPES pH 7.4) for 1 hour at 37°C in darkness. Coverslips were then mounted in an imaging chamber continuously perfused (1 ml/min) with HBSS at ~22°C using a multibarreled gravity-driven, automatic operated perfusion system.

TRPV1 activity was evoked with a first 15-s pulse of capsaicin 0.01, 0.1, 1 and 10 μM and a second 15 s pulse of a supramaximal concentration of capsaicin (100 μM) after a 5-minutes washing with HBSS. The same protocol was applied for DRG cultures plus an additional brief (15 s) application of 40 mM KCl to distinguish neurons from non-neuronal cells and to ensure that cells were healthy and responsive. Fluorescence from individual cells was monitored as a function of time and measured with a Zeiss Axiovert 200 inverted microscope (Carl Zeiss) fitted with an ORCA-ER CCD camera (Hamamatsu Photonics) through a 10× or 20× air objective. Fluo-4 was excited at 500 nm using a computer-controlled Lambda-10-2 filter wheel (Sutter Instruments), and emitted fluorescence was filtered with a 535-nm long-pass filter. Images were acquired and processed with

AquaCosmos package software (Hamamatsu Photonics). The amplitude of Ca^{2+} increase caused by stimulation with capsaicin was measured by subtracting the basal fluorescence (before capsaicin application) to the peak of fluorescence observed after capsaicin application. All data were expressed as means ± SEM, with n=number of cells tested and N=number of experiments realized. Statistical analysis was performed by two-way ANOVA, followed by Bonferroni post-test and significance level was preset to $p<0.05$.

2.15 Calcium microfluorographic assay

F11 cells were seeded in black 96 well plate with clear flat bottom and transfected with rat TRPV1 and Whirlin cDNAs and/or previously described siRNA. After 48 h cells were incubated with 100 μl of dye loading solution (1× HBSS, 20mM HEPES, pH 7.4), containing the fluorescence calcium indicator Fluo4-NW (Molecular Probes) and 2.5 mM probenecid, for 45 min at 37°C and 10 min at room temperature. Through the microplate reader POLARstar Omega (BMG Labtech) the Fluo-4 fluorescence signal (excitation at 494 nm and emission at 516 nm) was measured during 18 cycles. TRPV1 activity was evoked by the addition of 100 μM capsaicin in the fifth cycle using the injection system of the plate reader. We quantified the response to capsaicin by calculating the Area under the curve (AUC) between the fifth and the eighteenth cycles, generated by the increase of fluorescence signal induced by the response to capsaicin.

2.16 Electrophysiology

HEK293 cells were cotransfected with a mixture of TRPV1, Whirlin-myc, and CD8 (as a reporter) cDNAs, in a 2:2:1 ratio, and cultured for 48 h before being tested. In control samples, Whirlin was replaced by YFP. For selection, cells were incubated with 1 μl of anti-CD8-coated magnetic beads (Dynal). Patch pipettes (1.5 mm external and 1 mm internal diameter) were prepared from thin-borosilicate glass (World Precision Instruments) with a P-97 horizontal puller (Sutter Instruments) and fire-polished with a microforge MF-830 (Narishige) to have a final resistance of 2–3 MΩ. Standard whole-cell voltage-clamp protocols were applied using an EPC-10 amplifier (HEKA Electronic). Pipettes were filled with standard internal solution containing (in mM): 144 KCl, 2 $MgCl_2$, 5 EGTA and 10 HEPES. The pH was adjusted to 7.2 with KOH and the osmolarity set to 295 mosmol/kg. Standard extracellular solution contained (in mM): 140 NaCl, 4 KCl, 2 $CaCl_2$, 2 $MgCl_2$, 10 HEPES, 5 glucose and 20 mannitol. The pH was adjusted to 7.4 and the osmolarity set to 320 mosmol/kg. For acid solution, HEPES was replaced with MES and pH adjusted to 6. The different saline solutions were applied with a gravity-driven local microperfusion system with a rate flow of about 500 μl/minute located within about 300 μm of cell under study. Capsaicin stock (100 mM) was prepared in DMSO and diluted as indicated for the experiments in bath solution the day of the experiment. All recordings were performed at room temperature (22–24°C).

Voltage-step protocols consisting of 100 ms depolarizing pulses from −120 mV to +220 mV in steps of 20 mV were used. The holding potential (V_h) was 0 mV and the time interval between each pulse was 5 s. The conductance-voltage (G–V) curves were obtained by converting the maximal current values from the voltage step protocol to conductance using the relation $G=I/(V-V_R)$, were G is the conductance, I is the peak current, V is the command

pulse potential, and VR is the reversal potential of the ionic current. G–V curves for each cell were fitted to the Boltzmann equation: $G=G_{max}/1 + \exp[z_g(V-V_{0.5})/kT]$, where G_{max} is the maximal conductance, $V_{0.5}$ is the voltage required to activate the half-maximal conductance, and z_g is the gating valence. Thereafter, estimated G_{max} values were used to obtain the normalized G/G_{max}-V curves.

Capsaicin- or acidic pH-evoked currents were elicited with V_h set at −60 mV. Pulses were applied for a time sufficient for the response to reach plateau. Current density was calculated by dividing the whole-cell current by the cell capacitance. Data were visualized and analyzed using PulseFit (HEKA Electronic), GraphPad Prism 5 statistical software (GraphPad Software) and Origin 8.0 (OriginLab Corporation). All data were expressed as means±SEM, with n=number of cells tested. For statistical analysis, the unpaired *t* test was applied and significance level was preset to $p<0.05$.

3. Results

3.1 Whirlin interacts with TRPV1

A yeast two-hybrid screen, using the cytosolic N-end domain of TRPV1 as bait (16), identified, among others, the cytoskeletal Whirlin/CIP98/DFNB31 as a potential TRPV1 interacting protein. Whirlin is a PDZ-scaffold protein that plays a pivotal functional role in retinal photoreceptors and in vestibular and cochlear hair cells (20,26,31), as well as it contributes to mechanosensory transduction in proprioceptors (24).

The interaction of both proteins was confirmed *in vitro* with pull-down experiments using bacterially expressed GST-NtTRPV1. This recombinant protein pulled down Whirlin-myc from a HEK293 extract expressing the PDZ-scaffold protein (Fig. 1A), suggesting an interaction of TRPV1 ankyrin domains and the whirlin PDZ domains. We next evaluated whether Whirlin-myc interacted with TRPV1 full-length in cells using a co-immunopurification strategy. As illustrated in Figure 1B, an anti-myc monoclonal antibody co-immunoprecipitated Whirlin-myc and TRPV1 from a whole HEK293 cell extract containing both proteins. Similarly, we could immunoprecipitate Whirlin-myc using a polyclonal anti-HA antibody to immunoprecipitate HA-TRPV1 (Supplemental information, Fig. S1), corroborating that both proteins complex when co-expressed in cells. Furthermore, TRPV1 was also able to associate with PSD95 another protein having PDZ domains (Fig. 1B). We identified a potential PDZ internal ligand in the C-end of TRPV1 (SMV at amino acids 832 to 834), but found that deletion of this sequence did not affect whirlin binding to TRPV1 (Fig. 1B, V-stop line). Collectively, these results indicate a putative, non-canonical interaction of TRPV1 N-terminus, presumably by the ankyrin repeats and PDZ domains.

Structurally, Whirlin displays two PDZ domains at the N-terminus, a third one at the C-end, and a Proline-rich region between the second and third PDZ domains (20). Thus, we questioned which of the PDZ domains mediated the interaction with TRPV1. To address this question, we truncated Whirlin in two segments, one encompassing the PDZ1 and PDZ2 domains (PDZ1+2-myc), and the other containing the Pro-rich region and the PDZ3 (PDZ3-myc). These truncations were co-expressed with TRPV1 in HEK293 cells for co-immunopurification assays. Notably, both truncated proteins were able to strongly bind and

immunopurify TRPV1 (Fig. 1C), indicating that the interaction of Whirlin with the thermoTRP can be sustained by the three PDZ domains. This result is relevant since Whirlin is expressed as long and short isoforms resulting from splicing (32). Taking together, these results indicate that TRPV1 and Whirlin can form a stable complex in cells that implies an interaction of TRPV1 N-terminus and Whirlin PDZ domains.

To investigate the physiological relevance of TRPV1-Whirlin association, we determined whether both proteins co-localize in sensory neurons. First, we checked that DRG neurons in culture express Whirlin. For this purpose, we used qPCR to amplify Whirlin mRNA and western immunoblots to detect protein expression. Both techniques readily detected the presence of Whirlin in primary cultures of rat sensory neurons (Supplemental information, Fig. S2). Second, we used immunocytochemistry to evaluate if Whirlin and TRPV1 co-express in the same neurons. As depicted in Figures 1D and E, both proteins were present in nociceptors from neonatal rat and adult mouse DRGs (Supplementary information, Fig. S3). In primary cultures of nociceptors, Whirlin and TRPV1 displayed a cortical co-localization in the neuronal soma (Figs. 1D and E). Third, we employed immunohistochemistry to investigate the presence of both proteins in DRG cryo-sections (Supplementary information, Figs. S4–S6). This analysis detected the presence of Whirlin in 55% of peripheral fibers, including C-type (peptidergic and non-peptidergic sensory neurons) and A-type fibers (Table I), substantiating the presence of whirlin in peripheral sensory neurons (24). Around 70% of the Whirlin positive fibers also expressed TRPV1 (Table I). Therefore, these observations imply that Whirlin and TRPV1 are present in DRG neurons and appear to be part of a protein complex.

3.2 Whirlin increases TRPV1 expression

Having confirmed the association of TRPV1 and Whirlin in cells and neurons, we next investigated the influence of PDZ-scaffold protein in TRPV1 expression. For this purpose, both proteins were co-transfected into HEK293 cells and the expression level of TRPV1 was determined by western immunoblot at 48h. As shown in Figure 2A, an increment in Whirlin expression levels resulted in a dose-dependent increment of TRPV1 expression up to ~2-fold at a TRPV1:Whirlin-myc cDNAs ratio of 1:2 (Fig. 2B). This increment was also discernible at 24h after transfection (Supplementary information, Fig. S7A). A similar result was observed when Whirlin-myc was transfected into a cell line that stably expresses TRPV1 (Supplementary information, Fig. S7B), and into primary nociceptor cultures (Fig. 2C). Overexpression of Whirlin in nociceptors resulted in a significant 1.4-fold increment of TRPV1 expression (Fig. 2D). Therefore, a notable effect of Whirlin expression is to increase the total expression of TRPV1.

Subsequently, we evaluated if the higher levels of TRPV1 observed when co-expressed with Whirlin also resulted in a higher delivery and insertion into the plasma membrane. For this purpose, we evaluated the receptor surface expression by biotinylation of membrane-expressed proteins. Noteworthy, as shown in Figs. 2E and F, Whirlin produced a notable 2-fold increment in the localization of TRPV1 at the plasma membrane that parallels the higher expression of the channel induced by the cytoskeletal protein. This result was further substantiated in intact non permeabilized cells using the TRPV1e antibody that recognizes

an extracellular epitope (7). Sequential labeling with TRPV1e and then against the Whirlin-myc protein (α-myc) clearly show an increase in membrane TRPV1 levels and cortical co-localization with Whirlin (Fig. 2G). The higher TRPV1 levels at the plasma membrane promoted by Whirling appear forming large receptor clusters, as evidenced by the enhanced clustered YFP-TRPV1 membrane labelling in the presence of the PDZ scaffold protein (Fig. 2H). Therefore, these results indicate that Whirlin is a PDZ-scaffold protein that increases the membrane localization of TRPV1 in cells, and appears to promote receptor clustering.

3.3 Overexpression of Whirlin marginally modulates TRPV1 channel activity

Because Whirlin increases the expression of TRPV1, we next functionally evaluated the effect of whirlin on TRPV1 channel activity by patch clamp and Ca^{2+} imaging. Surprisingly, Whirlin reduced, rather than increased, the magnitude of the voltage-evoked TRPV1 ionic currents (Fig. 3A), as clearly evidenced by the decrease in the current density at high depolarizing potential (Fig. 3B). The kinetics of the ionic currents was virtually identical in cells expressing only TRPV1 and those co-expressing the channel and Whirlin (Fig. 3A). Analysis of the conductance-to-voltage relationships revealed that the voltage dependence of channel gating was slightly shifted to higher voltages in the presence of Whirlin (Fig. 3C), indicating that the energetics of channel gating was marginally increased ($V_{0.5}$=96±2 mV and $V_{0.5}$=117±3 mV in the absence and presence of Whirlin, respectively). Conversely, the PDZ-scaffold protein did not alter TRPV1 voltage sensitivity, as evidenced by similar gating valence of the gating process (0.55±0.03 and 0.58±0.02 in the absence and presence of Whirlin, respectively).

We also examined channel gating evoked by mild acidic extracellular pH and capsaicin. Akin to voltage-induced gating, Figures 3D and F show a modest decrease in pH-gated TRPV1 currents at negative potentials when Whirlin was co-expressed with the thermoTRP. In contrast, Whirlin expression did not significantly affect the magnitude of the capsaicin-activated ionic currents (Figs. 3E and G), nor capsaicin-induced Ca^{2+} influx (Figs. 3H–J). The apparently milder impact of Whirlin on capsaicin responses may be due to its stronger activating potency than voltage and pH, which are considered partial activators (4,33). Taken together, these results imply that heterologous co-expression of Whirlin with TRPV1 in HEK293 cells does not increase TRPV1 channel activity, but rather marginally decreases the channel functionality. This finding is consistent with the clustering of TRPV1 induced by Whirlin (Fig. 2H), as TRPV1 clustering has been reported to negatively modulate channel function (29).

3.4 Silencing of Whirlin expression reduces TRPV1 cellular expression and function

We next evaluated the functional consequences of abrogating Whirlin expression using specific siRNAs. For this purpose, we first used F11 cells (34). Because F11 cells do not express Whirlin nor TRPV1, we transfected them with both proteins. Twenty-four hours later, these cells were re-transfected with one or a mix of the three siRNAs designed against Whirlin, and the expression of both proteins was evaluated by western immunoblot. As illustrated in Figure 4A, the three individual siRNAs significantly reduced Whirlin protein levels. This decrease was concomitant with a reduction in Whirlin mRNA (data not shown). Notably, down regulation of Whirlin expression with siRNAs resulted also in a significant

decrement of TRPV1 protein levels in F11 cells co-transfected with TRPV1 and Whirlin (Fig. 4A). This reduction is more evident for siRNA-1 and siRNA-2 than for siRNA-3. As expected, transfection of these siRNAs against Whirlin significantly reduced TRPV1 levels and, concomitantly, the extent of capsaicin-evoked Ca^{2+} responses in F11 cells co-expressing both proteins (Supplemental information, Fig. S8). Since the three siRNAs display a similar functional effect, we selected the siRNA–2 for the next experiments.

Immunocytochemical exploration of Whirlin and TRPV1 levels in F11 cells in culture substantiated the effect of siRNA-2 on TRPV1 levels obtained with western immunoblots. As illustrated in Figure 4C, Whirlin and TRPV1 co-localized in the same cells (top panel). Transfection with a scrambled siRNA (sc-siRNA) did not affect the expression of Whirlin nor TRPV1 (Fig. 4B, bottom panel). In marked contrast, transfection of siRNA-2 downregulated the expression of Whirlin and, concomitantly, virtually silenced the expression of TRPV1 (Fig. 4C, top panel). This result suggests that inhibition of Whirlin synthesis by siRNA-2 results in a net degradation of both proteins, presumably through the proteasome. To test this hypothesis, after transfecting the siRNA into cells expressing both proteins, we incubated these cells with the proteasomal inhibitor MG132 and examined the expression of Whirlin and TRPV1 by immunocytochemistry. Noteworthy, inhibition of proteasome activity prevented the degradation of Whirlin and maintained the expression level of TRPV1 in cells transfected with the siRNA-2 (Fig. 4C, bottom panel).

To examine the functional effect of Whirlin knockdown, we evaluated TRPV1 activity by Ca^{2+} microfluorography using Fluo4 as Ca^{2+}dye. Figure 4E shows that transfection of F11 cells expressing Whirlin and TRPV1 with siRNA-2 resulted in lower capsaicin response due to the decreased expression levels of TRPV1. siRNA-2 effect on TRPV1 expression required the presence of Whirlin as it was ineffective in control F11 cells that were not transfected with the PDZ-scaffolding protein, substantiating the stabilizing effect of Whirlin on TRPV1 expression. Furthermore, it was sequence specific since the scrambled sc-siRNA did not affect TRPV1 expression levels nor activity (Fig. 4D). Notably, inhibition of proteasome activity with MG132, which prevents the degradation of expressed Whirlin and TRPV1 (Fig. 4C, bottom panel), attenuated TRPV1 downregulation in cells transfected with siRNA2 (Fig. 4D). Collectively, these results suggest that Whirlin stabilized the cellular and membrane expression of TRPV1. Downregulation of the PDZ-scaffolding protein concomitantly reduced the cellular and membrane levels of the thermoTRP channel.

We next sought to investigate the consequences of silencing Whirlin in primary cultures of DRG neurons. For this purpose, primary cultures of nociceptors were transfected with siRNA-2 and the expression of Whirlin and TRPV1 was first investigated by immunocytochemistry (Fig. 5A). As siRNA control, we used sc-siRNA. Transfection of siRNA-2 in nociceptors in culture resulted in the virtual disappearance of Whirlin and the concomitant fading of TRPV1 levels. Akin to F11 cells, degradation of both proteins could be prevented by inhibition of the proteasome with MG132 (data not shown). To functionally investigate the effect of siRNA-2, we transfected the neurons with a Cy3-siRNA-2::siRNA-2 mixture or Cy3-sc-siRNA:sc-siRNA that allowed us to evaluate capsaicin-induced Ca^{2+} influx in transfected nociceptors (Fig. 5A). This was necessary because of the high heterogeneity in capsaicin responses of primary nociceptor cultures. Using this strategy, our

data revealed a significant decrease in the percentage of capsaicin responsive neurons in cultures transfected with siRNA-2, as compared with control and sc-siRNA-transfected neurons. However, the magnitude of the capsaicin-evoked Ca^{2+} responses in nociceptors was not significantly affected by siRNA-2 (data not shown), most likely because these responding neurons may not co-express Whirlin and TRPV1. This result was further confirmed by patch clamp experiments in nociceptive neurons in culture (Supplemental Figure S9). Therefore, downregulation of Whirlin expression in a subpopulation of sensory neurons results in a decrease of TRPV1 expression, substantiating the stabilization of TRPV1 expression by the cytoskeletal PDZ-scaffold protein.

3.5 Whirlin increased the stability of TRPV1 in cells

The effect of whirlin on TRPV1 cellular stability was investigated by monitoring the time course of the proteins cellular degradation upon inhibition of protein synthesis with cycloheximide (Figs. 6A and 6B). In the absence of Whirlin, TRPV1 is relatively stable, showing a slow degradation kinetics that reaches ≈40% elimination upon 24 h translational arrest. Unexpectedly, in the presence of Whirlin the receptor exhibited significantly faster elimination kinetics and higher degradation, as ≥80% of TRPV1 faded away after 24h (Fig. 6B). Noteworthy, the faster and more extensive TRPV1 degradation in the presence of Whirlin closely matches the kinetics of Whirlin elimination (Fig. 6B), suggesting a causal relation in the degradation of both proteins. Indeed, this result suggests that in the presence of Whirlin the elimination of the thermoTRP is driven by the PDZ-scaffold protein, and probably depicts the degradation of the protein complex. This finding is in agreement with the observed degradation of TRPV1 induced by silencing of Whirlin expression with siRNAs.

To further examine the effect of Whirlin on the cellular stability of TRPV1, we compared the expression levels of TRPV1 before and after inhibiting lysosomal and proteasomal degradation in the absence and presence of Whirlin. As illustrated in Figures 6C and D, inhibition of lysosomal activity with Leupeptin (L) did not affect the level of TRPV1 independently of the presence of Whirlin. In marked contrast, inhibition of the proteasome with Epoxomicin (E) significantly augmented the expression level of TRPV1 in the absence of Whirlin (Fig. 6D), implying that, under these conditions, TRPV1 turnover is mediated via the proteasome. In the presence of Whirlin, however, the proteasomal inhibitor did not affect the level of channel expression (Fig. 6D), suggesting a lower turnover of the receptor in the presence of the PDZ-scaffold protein. Taken together, these results strongly suggests that Whirlin reduced the amount of channel protein being degraded, implying a stabilization of TRPV1 expression by the PDZ-scaffold protein.

We have previously reported that degradation of TRPV1 can be evoked by long exposure of the receptor to capsaicin, a process that targets the thermoTRP to lysosomal degradation (35). Thus, we next hypothesized that Whirlin-mediated stabilization of TRPV1 cellular expression may also reduce the extension of vanilloid-induced receptor internalization and degradation. Accordingly, we next investigated the effect of Whirlin on agonist-evoked receptor elimination and evaluated the levels of TRPV1 upon prolonged exposure to capsaicin in the absence and presence of Whirlin. As depicted in Fig. 6E, in the absence of

Whirlin, 20 min incubation with capsaicin of cells expressing TRPV1 produced a 60% decrease in the receptor expression. In contrast, in the presence of Whirlin, this reduction was significantly lower (Fig. 6F), consistent with a higher cellular stability of TRPV1 in the presence of the PDZ-scaffold protein that can even partially reduce vanilloid-induced lysosomal degradation of TRPV1. Collectively, all these results indicate that the main effect of Whirlin-TRPV1 interaction is to augment the stability of TRPV1, most likely by increasing its membrane stability.

4. Discussion

The activity of ion channels, including thermoTRPs, depends on the interaction of these membrane proteins with a plethora of partners that ensure their proper cellular activity. Analysis of the TRPV1 channelosome or singalplex has identified thus far protein partners mainly involved in receptor trafficking, delivery and clustering into the plasma membrane, as well as proteins that modulate its channel activity (16,29,36). Furthermore, interfering with receptor membrane delivery has resulted in a useful pharmacological approach to understand the contribution of TRPV1 pathological recruitment to pain transduction (7), and a therapeutic strategy to reduce pain signaling (37). Therefore, unveiling the components of the TRPV1 signalplex is important for understanding the intricacies of the receptor pathophysiological regulation. Indeed, identification of these protein complexes may provide new therapeutic targets for drug intervention.

By using a yeast two-hybrid approach, we have identified Whirlin, a PDZ-scaffold protein, as an interacting partner of TRPV1. In humans, Whirlin is encoded by the gene *Deafness autosomal recessive 31*, which is pivotal for retinal photoreceptor and vestibular and cochlear hair cells function (38,39). Indeed, mutations in this gene have been associated with autosomal recessive non-syndromic deafness and the Usher Syndrome (22,23). Additionally, this protein has been also implicated in mechanotransduction, a role recently substantiated by virtue of its location in peripheral proprioceptors where it facilitates afferent firing in response to muscle stretch (24). Whirlin was initially identified as a CASK interacting protein (CIP98), a member of the MAGUK protein family that plays important roles in the molecular organization of synaptic proteins in the central nervous system (21). Thus, Whirlin, as other PDZ-scaffold proteins, may be essential for the assembly and stabilization of protein networks in synapses (40), as well as in peripheral sensory endings of proprioceptive neurons (24). Our finding that Whirlin interacts with TPRV1 in peripheral nociceptors further substantiates a significant role of this protein in sensory transduction. Indeed, we found that Whirlin isoforms (long and short) form a stable complex with the N-terminal domain of TRPV1. Notably, this complex appears mediated by non-canonical PDZ interactions (41), as TRPV1 does not display a PDZ ligand in the N-terminus domain. Thus, the assembly of both proteins seems mainly due to the binding of the ankyrin and PDZ domains.

The most salient contribution of our study is that Whirlin associates with TRPV1 and increases the expression level and the stability of TRPV1. In transfected cell lines, the heterologous co-expression of Whirlin with TRPV1 augmented the expression of the receptor, as well as its delivery to the plasma membrane. A similar result was obtained when

the PDZ-scaffold protein was overexpressed in primary cultures of rat sensory neurons. Intriguingly, however, the larger TRPV1 expression in the presence of Whirlin did not result in a concomitant increase in channel activity suggesting that the PDZ-scaffold protein may exert a direct or indirect inhibitory action on TRPV1 channel activity. Although it is normally expected that an increase in protein expression leads to higher activity, it must be also noticed that increasing the membrane expression of a channel protein may induce its clustering, which could be detrimental for channel activity as clustered channels may exhibit impaired gating. In support of this tenet, we previously demonstrated that GABARAP-induced clustering of TRPV1 in the cell membrane resulted in a decrease of channel activity, even though GABARAP notably augmented the total and membrane expressed TRPV1 (29). Here, we noticed that whirlin increased TRPV1 clustering in the cell membrane, thus providing an explanation for the apparent lower channel activity of receptor in the presence of the PDZ scaffold protein. A recent study on the spatiotemporal organization of TRPV1 in live cell membranes show the existence of three dynamic channel populations, one of them bound to microtubules (42). This cytoskeletal population appears as large clusters (860 nm) of slow mobility. It is tempting to speculate that whirlin, as well as GABARAP (29), may favor the formation of this clustered receptor population. In support of this tenet, whirlin reduced capsaicin-induced TRPV1 internalization, a process that has been associated to the channel subpopulation bound to caveolin-1 (29).

A more discernible effect on TRPV1 function was obtained when Whirlin expression was reduced using a specific siRNA. In recombinant F11 cells co-expressing Whirlin and TRPV1, knockdown of Whirlin expression notably reduced the expression level of TRPV1 and significantly decreased capsaicin-activated responses. Inhibiting the proteasome activity, a strategy that prevented the degradation of both Whirlin and TRPV1, preserved TRPV1 expression and vanilloid responses in these cells. Furthermore, treatment of primary cultures of nociceptors with Whirlin siRNA, also decreased the expression of TRPV1 and decreased the percentage of neurons responding to capsaicin. Taken together, these results indicate that Whirlin complexes with TRPV1 and stabilizes the expression of the vanilloid receptor. Silencing the expression of the PDZ-scaffold protein then results in a lower stability of TRPV1 that is eliminated concomitantly with Whirlin through proteasomal degradation.

It is intriguing that TRPV1 cellular stabilization is only observed when Whirlin is co-expressed with TRPV1, as TRPV1 is quite stable in cells in the absence of Whirlin. Furthermore, elimination of Whirlin in nociceptors in culture only affected the percentage of neurons responding to capsaicin but not the magnitude of the vanilloid-induced responses. These observations suggest that what is likely degraded in cells expressing both proteins is the Whirlin-TRPV1 complex. In support of this tenet, TRPV1 degradation upon treating the cells with cycloheximide follows an elimination kinetics virtually identical to that of Whirlin in cells where both proteins are co-expressed, and it is significantly faster and more extensive than that where only TRPV1 is expressed. This result implies that, in the presence of Whirlin, the stability of TRPV1 is primarily determined by formation of the Whirlin-TRPV1 complex. Taken together, Whirlin appears to form a stable complex with TRPV1 that increases the cellular stability of the thermoTRP. Additional support for this notion is provided by the lower internalization and degradation of TRPV1 induced by prolonged exposure of the receptor to capsaicin in the presence of Whirlin.

Mutations in the human Whirlin gene are responsible for autosomal recessive deafness DFNB31 and in cases of Usher syndrome type 2D in humans, and for the deafness phenotype in the Whirler mouse (20,22,23). Genetically, the mutation in the Whirler mice consists of a 592 bp deletion that leads to a truncation of the long isoform before the third PDZ and encompasses the first methionine of the short isoform (20). A question that arises is whether the Whirler mouse displays nociception abnormalities due to destabilization of the Whirlin-TRPV1 complex because of the truncation of Whirlin. Notably, we did not observe any significant nociceptive impairment in Whirler mice as compared with wild type littermates (Supplementary Table S1). Similarly, we did not detect any noticeable nociceptive deficit in a Whirlin transgenic mouse ($Whirlin^{neo/neo}$) that does not express the long isoform of the PDZ protein (Supplementary Table S2) (26). These results are consistent with our observation that TRPV1 is able also to interact with the PDZ1/2 and PDZ3 domains, suggesting an interaction with the long and short isoforms of the PDZ-scaffold protein. Indeed, the whirler and $Whirlin^{neo/neo}$ mice exhibit a similar distribution of TRPV1 in sensory fibers (Table I and Supplementary Figs. S10–S15). Thus, the lack of nociceptive impact observed in Whirler and $Whirlin^{neo/neo}$ mice may be due to the complexation and stabilization of TRPV1 with the short Whirlin isoforms expressed by nociceptors of these animals. Notably, an alternative Whirlin transgenic mouse, produced using a genome-wide knockout generation approach and characterized using systematic phenotyping, exhibited an increased thermal nociceptive threshold in the hot plate test (43), consistent with a defect in the activity of TRPV1 receptors in the peripheral terminals of these animals. Nevertheless, additional nociceptive characterization of these transgenic mice appears necessary to unveil the pathophysiological role of Whirlin-TRPV1 complex in nociceptive and pain signaling.

In conclusion, we have described that TRPV1 interacts with Whirlin, a cytoskeletal PDZ-scaffold protein, in nociceptors. The main functional role of the TRPV1-Whirlin complex is to stabilize the total and membrane expression of TRPV1, most likely in the peripheral terminals. Because the interaction of Whirlin with TRPV1 involves the ankyrin domains, it is plausible that the PDZ-scaffold protein also associates with other ankyrin-containing TRP channels, thus providing a mechanism to assemble and stabilize these channels in the peripheral nociceptive and propioceptive terminals. It would be also interesting to know if other TRP channels also interact with Whirlin, and if they contribute to define the phenotype characteristic of Whirlin mutants, namely deafness and the Usher syndrome. Although additional experimental support is needed to better understand the role of Whirlin assembling TRPV1 channels and nociceptor peripheral terminals, our data suggest that disruption of its interaction with TRPV1 may provide a novel pharmacological intervention to attenuate TRPV1 dysfunction in peripheral painful syndromes. Because full pharmacological abrogation of TRPV1 channel activity has not delivered yet a clinically useful approach due to unwanted side effects, exploration of alternative therapeutic approaches directed to modulate TRPV1 expression levels may lead to compounds with higher therapeutic index.

Supplementary Material

Refer to Web version on PubMed Central for supplementary material.

Acknowledgments

We thank Prof. D. Julius for kindly providing the rat TRPV1 cDNA and Dr. P Mburu for providing the whirler mouse. This work has been supported by grants from the Spanish Ministerio de Economía y Competitividad (MINECO) (BFU2012-39092-C02-01 to AFM and, the CONSOLIDER-INGENIO 2010 Program (CSD2008-00005 to AFM), and the Generalitat Valenciana PROMETEO/2014/011 and ISIC/2012/009 to AFM.

Reference List

1. Jara-Oseguera, As, Nieto-Posadas, As, Szallasi, A., Isias, LnD, Rosenbaum, T. Open Pain J. 2010; 3:68–81.
2. Caterina MJ, Schumacher MA, Tominaga M, Rosen TA, Levine JD, Julius D. Nature. 1997; 389:816–824. [PubMed: 9349813]
3. Voets T, Droogmans G, Wissenbach U, Janssens A, Flockerzi V, Nilius B. Nature. 2004; 430:748–754. [PubMed: 15306801]
4. Tominaga M, Caterina MJ, Malmberg AB, Rosen TA, Gilbert H, Skinner K, Raumann BE, Basbaum AI, Julius D. Neuron. 1998; 21:531–543. [PubMed: 9768840]
5. Planells-Cases R, Garcia-Sanz N, Morenilla-Palao C, Ferrer-Montiel A. Pflugers Arch. 2005; 451:151–159. [PubMed: 15909179]
6. Bhave G, Gereau RW. J Neurobiol. 2004; 61:88–106. [PubMed: 15362155]
7. Camprubi-Robles M, Planells-Cases R, Ferrer-Montiel A. FASEB J. 2009; 23:3722–3733. [PubMed: 19584302]
8. Jara-Oseguera A, Simon SA, Rosenbaum T. Curr Mol Pharmacol. 2008; 1:255–269. [PubMed: 20021438]
9. Gunthorpe MJ, Chizh BA. Drug Discov Today. 2009; 14:56–67. [PubMed: 19063991]
10. Gavva NR, Treanor JJ, Garami A, Fang L, Surapaneni S, Akrami A, Alvarez F, Bak A, Darling M, Gore A, Jang GR, Kesslak JP, Ni L, Norman MH, Palluconi G, Rose MJ, Salfi M, Tan E, Romanovsky AA, Banfield C, Davar G. Pain. 2008; 136:202–210. [PubMed: 18337008]
11. Kedei N, Szabo T, Lile JD, Treanor JJ, Olah Z, Iadarola MJ, Blumberg PM. J Biol Chem. 2001; 276:28613–28619. [PubMed: 11358970]
12. Owsianik G, Talavera K, Voets T, Nilius B. Annu Rev Physiol. 2006; 68:685–717. [PubMed: 16460288]
13. Garcia-Sanz N, Fernandez-Carvajal A, Morenilla-Palao C, Planells-Cases R, Fajardo-Sanchez E, Fernandez-Ballester G, Ferrer-Montiel A. J Neurosci. 2004; 24:5307–5314. [PubMed: 15190102]
14. Vlachova V, Teisinger J, Susankova K, Lyfenko A, Ettrich R, Vyklicky L. J Neurosci. 2003; 23:1340–1350. [PubMed: 12598622]
15. Lishko PV, Procko E, Jin X, Phelps CB, Gaudet R. Neuron. 2007; 54:905–918. [PubMed: 17582331]
16. Morenilla-Palao C, Planells-Cases R, Garcia-Sanz N, Ferrer-Montiel A. J Biol Chem. 2004; 279:25665–25672. [PubMed: 15066994]
17. Neve KA. Mol Pharmacol. 2005; 68:275–278. [PubMed: 15923382]
18. Yap CC, Liang F, Yamazaki Y, Muto Y, Kishida H, Hayashida T, Hashikawa T, Yano R. J Neurochem. 2003; 85:123–134. [PubMed: 12641734]
19. Sheng M, Sala C. Annu Rev Neurosci. 2001; 24:1–29. [PubMed: 11283303]
20. Mburu P, Mustapha M, Varela A, Weil D, El-Amraoui A, Holme RH, Rump A, Hardisty RE, Blanchard S, Coimbra RS, Perfettini I, Parkinson N, Mallon AM, Glenister P, Rogers MJ, Paige AJ, Moir L, Clay J, Rosenthal A, Liu XZ, Blanco G, Steel KP, Petit C, Brown SD. Nat Genet. 2003; 34:421–428. [PubMed: 12833159]
21. Hsueh YP. Curr Med Chem. 2006; 13:1915–1927. [PubMed: 16842202]
22. Mustapha M, Chouery E, Chardenoux S, Naboulsi M, Paronnaud J, Lemainque A, Megarbane A, Loiselet J, Weil D, Lathrop M, Petit C. Eur J Hum Genet. 2002; 10:210–212. [PubMed: 11973626]
23. Ebermann I, Scholl HP, Issa PC, Becirovic E, Lamprecht J, Jurklies B, Mill+ín JM, Aller E, Mitter D, Bolz H. Human genetics. 2007; 121:203–211. [PubMed: 17171570]

24. de Nooij JC, Simon CM, Simon A, Doobar S, Steel KP, Banks RW, Mentis GZ, Bewick GS, Jessell TM. J Neurosci. 2015; 35:3073–3084. [PubMed: 25698744]
25. Cabedo H, Carteron C, Ferrer-Montiel A. J Biol Chem. 2004; 279:33623–33629. [PubMed: 15159404]
26. Yang J, Liu X, Zhao Y, Adamian M, Pawlyk B, Sun X, McMillan DR, Liberman MC, Li T. PLoS Genet. 2010; 6:e1000955. [PubMed: 20502675]
27. Green JA, Yang J, Grati M, Kachar B, Bhat MA. BMC Neurosci. 2013; 14:96. [PubMed: 24011083]
28. Devesa I, Ferrandiz-Huertas C, Mathivanan S, Wolf C, Lujan R, Changeux JP, Ferrer-Montiel A. Proc Natl Acad Sci U S A. 2014; 111:18345–18350. [PubMed: 25489075]
29. Lainez S, Valente P, Ontoria-Oviedo I, Estevez-Herrera J, Camprubi-Robles M, Ferrer-Montiel A, Planells-Cases R. FASEB J. 2010; 24:1958–1970. [PubMed: 20179142]
30. Goswami C, Dreger M, Otto H, Schwappach B, Hucho F. J Neurochem. 2006; 96:254–266. [PubMed: 16336230]
31. van WE, van der Zwaag B, Peters T, Zimmermann U, Te BH, Kersten FF, Marker T, Aller E, Hoefsloot LH, Cremers CW, Cremers FP, Wolfrum U, Knipper M, Roepman R, Kremer H. Hum Mol Genet. 2006; 15:751–765. [PubMed: 16434480]
32. Wright RN, Hong DH, Perkins B. Invest Ophthalmol Vis Sci. 2012; 53:1519–1529. [PubMed: 22323458]
33. Matta JA, Ahern GP. J Physiol. 2007; 585:469–482. [PubMed: 17932142]
34. Francel PC, Harris K, Smith M, Fishman MC, Dawson G, Miller RJ. J Neurochem. 1987; 48:1624–1631. [PubMed: 2435852]
35. Sanz-Salvador L, Andres-Borderia A, Ferrer-Montiel A, Planells-Cases R. J Biol Chem. 2012; 287:19462–19471. [PubMed: 22493457]
36. Kim AY, Tang Z, Liu Q, Patel KN, Maag D, Geng Y, Dong X. Cell. 2008; 133:475–485. [PubMed: 18455988]
37. Ponsati B, Carreno C, Curto-Reyes V, Valenzuela B, Duart MJ, Van den Nest W, Cauli O, Beltran B, Fernandez J, Borsini F, Caprioli A, Di SS, Veretchy M, Baamonde A, Menendez L, Barros F, de la Pena P, Borges R, Felipo V, Planells-Cases R, Ferrer-Montiel A. J Pharmacol Exp Ther. 2012; 341:634–645. [PubMed: 22393248]
38. Kikkawa Y, Mburu P, Morse S, Kominami R, Townsend S, Brown SD. Human molecular genetics. 2005; 14:391–400. [PubMed: 15590699]
39. Maerker T, van WE, Overlack N, Kersten FF, McGee J, Goldmann T, Sehn E, Roepman R, Walsh EJ, Kremer H, Wolfrum U. Hum Mol Genet. 2008; 17:71–86. [PubMed: 17906286]
40. Kim E, Sheng M. Nat Rev Neurosci. 2004; 5:771–781. [PubMed: 15378037]
41. Maekawa K, Imagawa N, Naito A, Harada S, Yoshie O, Takagi S. Biochem J. 1999; 337(Pt 2):179–184. [PubMed: 9882613]
42. Storti B, Di RC, Cardarelli F, Bizzarri R, Beltram F. PLoS One. 2015; 10:e0116900. [PubMed: 25764349]
43. White JK, Gerdin AK, Karp NA, Ryder E, Buljan M, Bussell JN, Salisbury J, Clare S, Ingham NJ, Podrini C, Houghton R, Estabel J, Bottomley JR, Melvin DG, Sunter D, Adams NC, Tannahill D, Logan DW, Macarthur DG, Flint J, Mahajan VB, Tsang SH, Smyth I, Watt FM, Skarnes WC, Dougan G, Adams DJ, Ramirez-Solis R, Bradley A, Steel KP. Cell. 2013; 154:452–464. [PubMed: 23870131]

Highlights

1. Whirlin complexes with TRPV1 in sensory neurons
2. Whirlin increases cellular expression and stability of TRPV1
3. Whirlin induces TRPV1 clustering in the cell membrane
4. Ablation of Whirlin increases TRPV1 cellular degradation
5. Whirlin-TRPV1 complex may be a novel therapeutic target

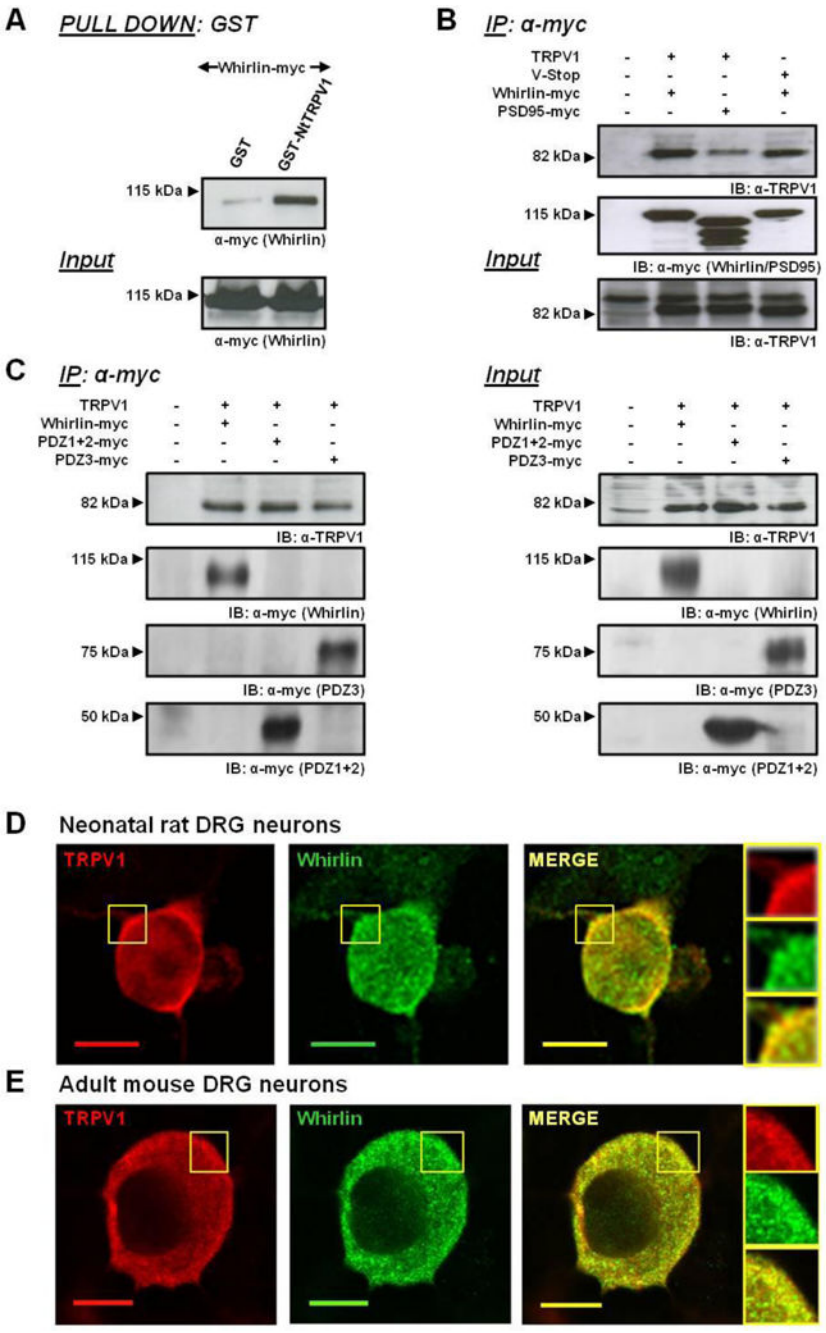

Figure 1. TRPV1 associates *in vitro* and *ex vivo* with Whirlin

(A) Pulldown assay using immobilized fusion protein between GST and the cytosolic TRPV1 Nt-domain (GST-Nt-TRPV1) associated a recombinant full-length Whirlin-myc produced in HEK293 cells. GST was used as a control. **(B)** Co-immunoprecipitation of transiently expressed TRPV1 full length, TRPV1 V-Stop (deletion 828–838 amino acids at the C-terminus or TRPV1) with Whirlin-myc or PSD95-myc proteins in HEK293 cells. **(C)** Co-immunoprecipitation of transiently expressed TRPV1 with whirlin-myc, PDZ1+2-myc and PDZ3-myc truncated forms of Whirlin in HEK293 cells. **(D, E)** Co-localization of endogenous TRPV1 and Whirlin expression in primary cultures of neonatal rat **(D)** or adult

mice **(E)** nociceptors by immunofluorescence. Left panel: TRPV1 labeled with anti-TRPV1 antibody (raised against an intracellular epitope; red). Middle panel: Whirlin antibody directed against a C-terminal epitope for rat and mouse DRGs, respectively (green). Right panel: overlay of TRPV1 and Whirlin immunoreactivities (yellow). Depicted squared regions are zoomed at the right side. Scale bar 10 μm.

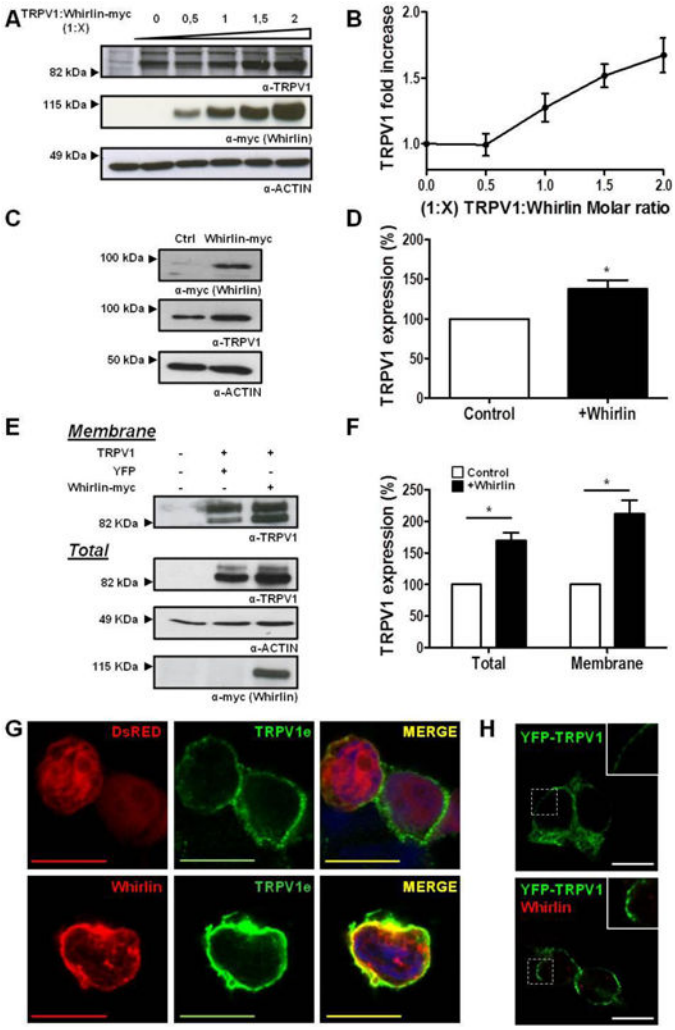

Figure 2. Whirlin expression enhances surface and total expression of TRPV1

(A, B) Representative immunoblot and quantification of HEK293 extracts transiently cotransfected with different molar ratios of TRPV1 and Whirlin-myc where a constant amount of TRPV1 was applied along with increasing whirlin-myc cDNA. TRPV1 appears as a double band depicting different glycosylated TRPV1 forms. Actin was used as loading control for normalization. **(C, D)** Representative immunoblot and quantification of neonatal rat DRG primary cultures electroporated with Whirlin-myc or YFP (as a control) cDNAs. **(E, F)** Representative immunoblot and quantification of surface expressed TRPV1 in HEK293 cells in the absence (YFP, control) or presence of Whirlin-myc. Surface proteins were separated by biotinylation, immunopurified with avidin and analyzed by immunoblot. Actin was used as loading control for normalization of total and membrane expressed protein. **(G)** Immunolabeling of non-permeabilized intact Control (TRPV1+DsRed) or Whirlin-transfected (TRPV1+Whirlin) cell membranes with anti-TRPV1e (green), an antibody that recognizes an extracellular epitope, and thereafter detergent-permeabilized for Whirlin staining (red). Cell nuclei were stained with DAPI (blue). **(H)** YFP-TRPV1 expression in HEK293 cells in the absence *(Top)* and presence of Whirlin *(Bottom).* Data

expressed as mean±SEM with N=5. *p<0.05 unpaired *t-Student* test. The inset denotes a 2× zoom of the squared area. Scale bars 10 μm.

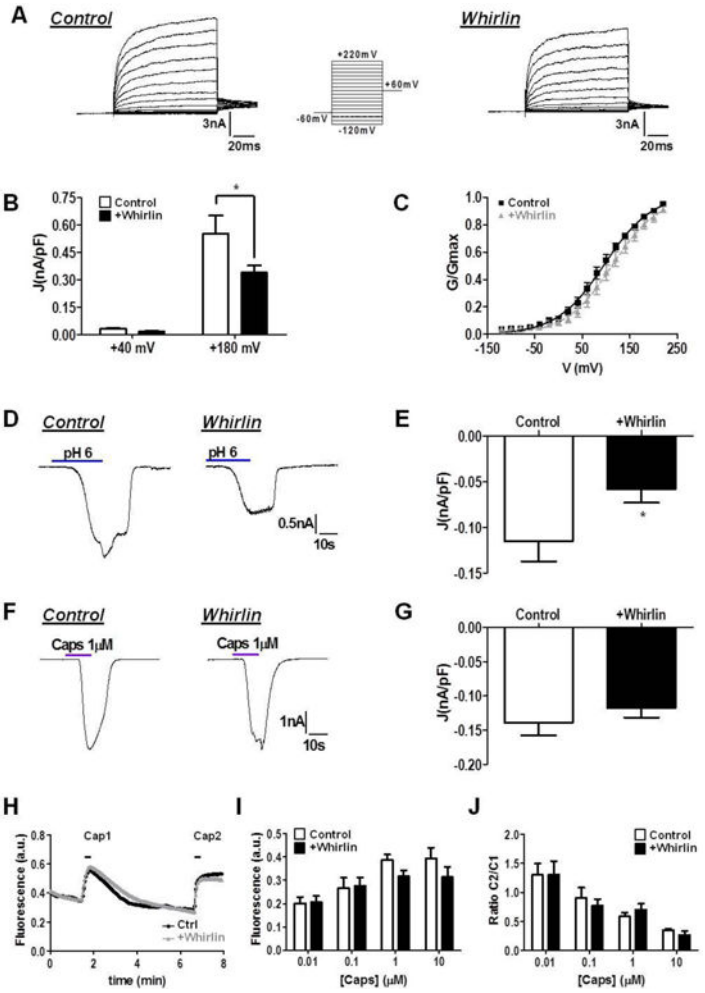

Figure 3. Effect of Whirlin on TRPV1 currents activated by voltage, acidic pH and capsaicin

(A) Representative family of ionic currents evoked by step potentials from −120 to +220 mV in 100 ms from V_h=0 mV in HEK293 cells transiently transfected with TRPV1 +YFP (Control) or TRPV1 +Whirlin. **(B)** Current densities (J, nA/pF) calculated from maximal currents at +40 mV and +180 mV. Data are shown as mean ± SEM with n=23 cells for each condition. *p<0.05, two-way ANOVA, Bonferroni post-test). **(C)** G–V relations for TRPV1 in the absence and presence of Whirlin. Conductance values were fitted to a normalized Boltzmann equation. $V_{0.5}$ values were 97±2 mV and 117±3 mV, and z_g values were 0.55±0.03 and 0.58±0.02, in the absence and presence of Whirlin, respectively. **(D)** Representative TRPV1 ionic current evoked by an extracellular acidic pH of 6.0 in the absence and presence of Whirlin. **(E)** The PDZ-scaffold protein decreases the magnitude of the acidic pH-activated TRPV1 ionic currents. **(F)** Representative TRPV1 ionic current evoked by 1 μM capsaicin in the absence and presence of Whirlin. **(G)** Capsaicin responses were not affected by the presence of Whirlin. For both conditions data are given as mean ±SEM, with n=21 for control cells and n≥22 for Whirlin expressing cells. *p<0.05 unpaired *t* test. **(H)** Representative capsaicin-induced Ca^{2+} fluxes in cells expressing TRPV1, and co-expressing TRPV1 and Whirlin. The first peak was evoked with 0.01 μM (Cap1), and the second with 100 μM (Cap2) capsaicin to get a saturated response. **(I)** Average peak

amplitude of the first vanilloid-activated Ca^{2+} response. au denotes arbitrary units **(J)** Ratio between the first and the second capsaicin-evoked Ca^{2+} responses. Data expressed as mean ±SEM with n›150 cells in each condition. No significant differences were detected using a Two-way ANOVA, followed by *Bonferroni post-test.*

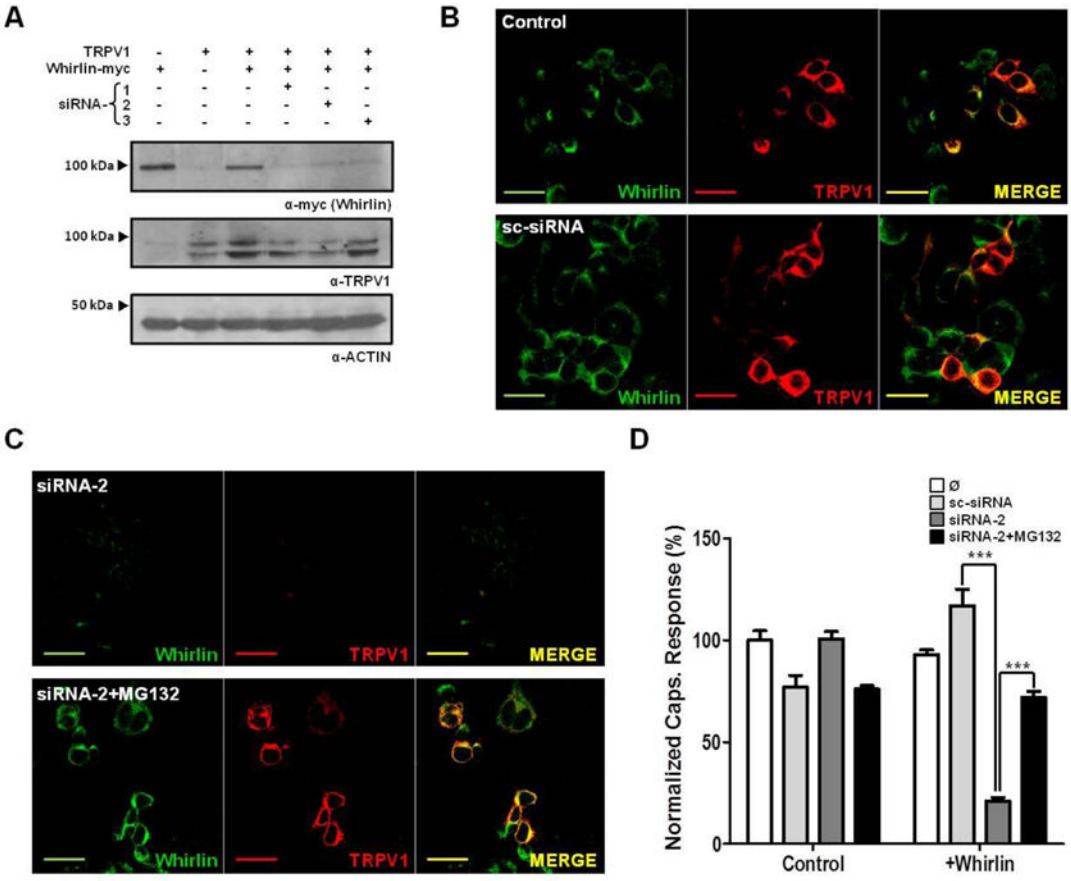

Figure 4. Silencing of Whirlin expression decreases TRPV1 cellular levels

(A) Immunoblots showing the effect of siRNAs against Whirlin on the levels of the PDZ-scaffold protein and TRPV1 transiently expressed in F11 cells. Three different siRNAs (siRNA-1, siRNA-2 and si-RNA-3) were used. **(B)** Immunocytochemical staining of F11 cells transiently co-expressing TRPV1 (red) and Whirlin (green) in control conditions and transfected with a scrambled siRNA (sc-siRNA). **(C)** Immunocytochemical staining of F11 cells transiently co-expressing TRPV1 (red) and Whirlin (green) transfected with siRNA-2 in the absence (Top) and presence of MG130 *(Bottom).* **(D)** Ca^{2+} microfluorographic assay in F11 cells expressing TRPV1 in presence or absence of Whirlin and transfected with sc-siRNA or siRNA-2. Ca^{2+} responses were evoked with a 100 μM capsaicin. Areas under curve (AUC) were calculated and normalized to the response of TRPV1-expressing F11 untreated cells (Ø). siRNAs were transfected at 50 nM, and proteasomal inhibition was carried out with 2 μM MG132. Data expressed as mean±SEM with N=5. *** $p<0.001$. Two-way ANOVA, followed by *Bonferroni post-test.* Scale bar 10 μm.

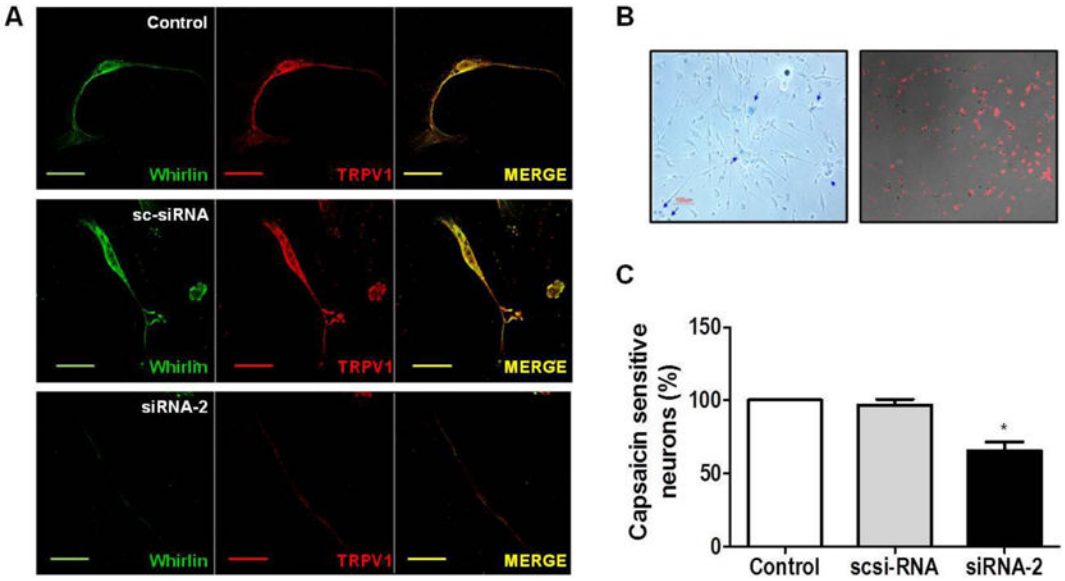

Figure 5. Silencing of Whirlin expression reduces TRPV1 neuronal levels and the number of capsaicin responding nociceptors

(A) Immunocytochemical TRPV1 (red) and Whirlin (green) staining of rat neonatal DRGs transfected with 50 nM siRNA-2 or sc-siRNA. Non-transfected cells were used as control. **(B)** Rat neonatal DRG cultures were transfected with a Cy3-labeled siRNA-2::siRNA-2 (1:10) to visualize transfected neurons. Trypan blue staining revealed a ~70% cell viability at 48 hours post transfection. **(C)** Percentage of Capsaicin responding neurons determined by Ca^{2+} imaging. Whirlin silencing was reduced the percentage of capsaicin sensitive neurons by ~40%. Capsaicin concentration used was 0.5 μM. Data are shown as mean ±SEM, with n≥165 neurons in three different experiments. * $p<0.05$ One way ANOVA, followed by *Bonferroni post-test.* Scale bar 10 μm.

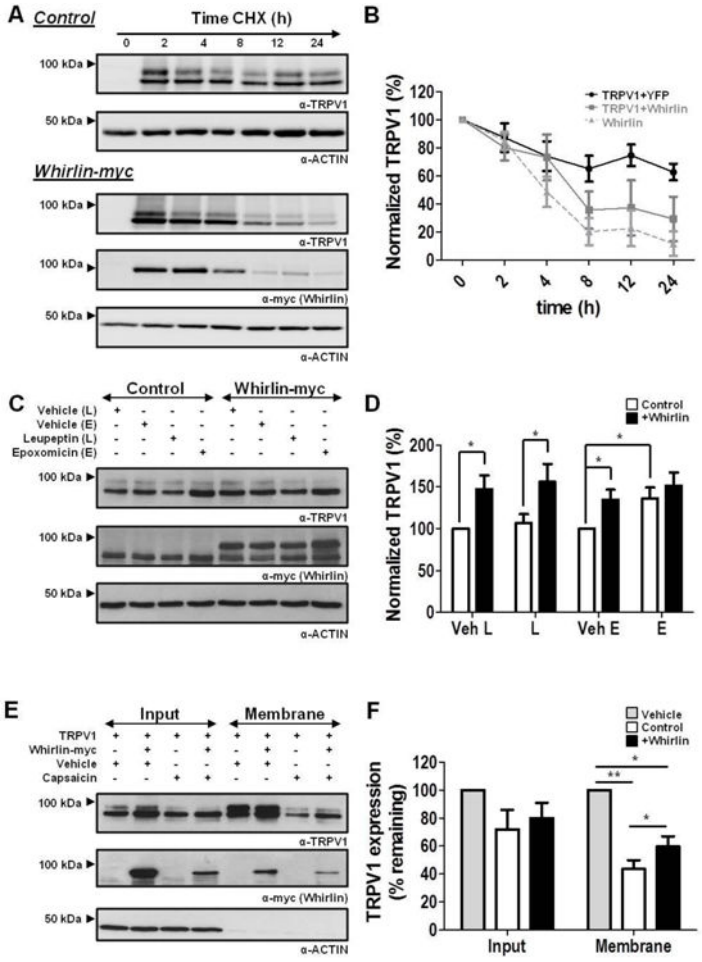

Figure 6. Effect of Whirlin on TRPV1 cellular and membrane levels

(A) Kinetics of TRPV1 and Whirlin-myc expression after arresting protein translation with 300 μg/ml cycloheximide (CHX) analyzed by western immunoblot of both proteins. **(B)** Quantitation of TRPV1 and Whirlin-myc protein normalized levels upon incubation with CHX. Quantitation was performed by digitizing the immunoblots. **(C)** Immunoblots showing the **e**ffect of Leupeptin (L) and Epoxomicin (E) on TRPV1 expression in the absence and presence of Whirlin-myc. **(D)** Quantitation of TRPV1 levels in the immunoblots depicted in panel C. Control depicts HEK293 cells co-transfected with TRPV1 and YFP. Whirlin-myc depicts HEK293 cells co-transfected with TRPV1 and Whirlin-myc. Cells were treated with 100 μM Leupeptin or 1 μM Epoxomicin, or their respective vehicles water (Veh-L) and DMSO (Veh-E) for 12h. **(E, F)** Representative immunoblots of the effect of 20 min capsaicin exposure on TRPV1 membrane levels in the absence and presence of Whirlin. HEK293 cells treated with 10 μM capsaicin or vehicle (DMSO) for 20 min at 37°C and, thereafter, biotinylated, avidin affinity purified and analyzed by western immunoblot. Data are given as mean±SEM with N=5. * $p<0.05$; ** $p<0.01$. Unpaired *t-Student test.*

Table I

TRPV1 coexpresses with Whirlin isoforms in sensory neurons.

	WT	Whirlin$^{neo/neo}$	Whirler
TRPV1$^+$	33 ± 1	31 ± 1	34 ± 1
TRPV1$^+$ × IB4$^+$	4 ± 1	6 ± 1	4 ± 1
TRPV1$^+$ × CGRP$^+$	50 ± 4	49 ± 3	40 ± 4
TRPV1$^+$ × NF200$^+$	11 ± 1	11 ± 2	11 ± 3
TRPV1$^+$ × Whirlin$^+$	64 ± 3	63 ± 4	49 ± 8
Whirlin$^+$	56 ± 1	51 ± 2	53 ± 1
Whirlin$^+$ × IB4$^+$	35 ± 2	35 ± 3	43 ± 5
Whirlin$^+$ × CGRP$^+$	43 ± 2	49 ± 6	53 ± 5
Whirlin$^+$ × NF200$^+$	41 ± 3	42 ± 4	31 ± 5
Whirlin$^+$ × TRPV1$^+$	40 ± 2	40 ± 3	31 ± 7

Immunohistochemistry was carried out on serial DRGs cryo-sections of 14 μm from wild type, whirler and whirlin$^{neo/neo}$ mice. Immunohistochemical staining was performed with polyclonal antibodies for TRPV1, Whirlin and the neuronal markers CGRP, IB4 and NF200. Data expressed mean ± SEM as percentage of total neurons analyzed per each section. Three animals and a minimum of 5 sections per group were analyzed.